Discovery and Mechanistic Investigation of Pt–Catalyzed Oxidative Homocoupling of Benzene with PhI(OAc)2

Journal:	*Dalton Transactions*
Manuscript ID	DT-ART-11-2019-004261.R1
Article Type:	Paper
Date Submitted by the Author:	28-Dec-2019
Complete List of Authors:	Nabavizadeh, S. Masoud; Shiraz University, Chemistry Niroomand Hosseini, Fatemeh; Islamic Azad University, Shiraz Branch, Chemistry, Chemistry Park, Chan; University of California, Chemistry and Biochemistry, and Chemical Engineering Wu, Guang; University of California, Santa Barbara, Chemistry & Biochemistry Abu-Omar, Mahdi; University of California, Chemistry and Biochemistry, and Chemical Engineering

SCHOLARONE™
Manuscripts

Discovery and Mechanistic Investigation of Pt-Catalyzed

Oxidative Homocoupling of Benzene with PhI(OAc)$_2$

S. Masoud Nabavizadeh,*[a,b] Fatemeh Niroomand Hosseini,[c] Chan Park,[b] Guang Wu[b] and

Mahdi M. Abu-Omar*[b]

[a]Professor Rashidi Laboratory of Organometallic Chemistry, Department of Chemistry, College of Sciences, Shiraz University, Shiraz 71467-13565, Iran. [b]Department of Chemistry and Biochemistry, University of California, Santa Barbara, Santa Barbara, California 93106, United States. [c]Department of Chemistry, Shiraz Branch, Islamic Azad University, Shiraz 71993–37635, Iran.

Corresponding Authors

S. Masoud Nabavizadeh: nabavizadeh@shirazu.ac.ir

Mahdi Abu-Omar: abuomar@chem.ucsb.edu

Abstract

We present a Pt-catalyzed direct coupling of benzene to biphenyl. This catalytic reaction employs the cyclometalated platinum(II) complex [PtMe(bhq)(SMe$_2$)] (bhq = benzo[h]quinolate) with PhI(OAc)$_2$ as oxidant and does not require an acid, a co-catalyst or a solvent. Reaction kinetics and characterization of potential catalytic species are reported. The reaction is first-order in Pt and second-order in benzene, which implicates the second C-H activation step as rate-determining. A Pt(II)/Pt(IV) catalytic cycle is suggested. The reaction commences by oxidation of the Pt(II) complex to give the platinum(IV) species [Pt(bhq)(SMe$_2$)(OAc)$_2$](OAc) followed by C-H activation of benzene to afford the

intermediate [PtPh(bhq)(SMe$_2$)(OAc)](OAc) concurrently with release of HOAc. A second benzene molecules reacts similarly to give the diphenyl intermediate [PtPh$_2$(bhq)(SMe$_2$)](OAc). C-C bond forming reductive elimination ensues to regenerate Pt(II) and complete catalytic cycle. The proposed mechanism has been examined by DFT computations, which provides support to experimental findings.

Introduction

Metal-catalyzed cross coupling of non-activated arenes has attracted much attention in recent years[1, 2] because of its application in organic synthesis and industrial chemistry.[3-12] Biphenyls are important in materials science as structural components. As a result, much has been published on $C_{sp^2} - C_{sp^2}$ bond forming reactions. In most reports a pre-activation step such as halogenation is necessary before the coupling reaction can ensue. In typical transformations, a transition metal catalyst is used for cross-coupling of an aryl halide and an arene.[1, 13] These reactions proceed in acidic solutions or in the presence of a co-catalyst/additive. Beside this synthetic strategy of using aryl halides,[14, 15] protocols for direct C-H coupling have also been reported using Pd,[16] Ru,[17] and other metal complexes[2] as catalyst. Although oxidative C-H coupling reactions are becoming more wide-spread in synthetic chemistry, mechanistic studies of benzene coupling to produce biphenyl remain rare.[1] Recent mechanistic studies by Stahl and co-workers on the homocoupling of o-xylene using Pd(OAc)$_2$ as catalyst and O$_2$ as oxidant are worthy of special mention.[10, 11]

Mechanistic understanding of the key catalytic steps can help in improving reaction conditions and discovery of new catalysts. Based on our previous studies of catalytic processes and their mechanisms,[18-20] we report herein on the first platinum-catalysed coupling of benzene to produce biphenyl. The catalytic system based on

[PtMe(bhq)(SMe$_2$)], **1**, (bhq = benzo[h]quinolate) pre-catalyst is characterized in detail using GC/MS, ^{1}H NMR, chemical kinetics and DFT. The results reveal a rate law that is first-order in Pt and second-order in benzene. When combined with characterization of Pt species along the catalytic cycle, the kinetic data suggests a mechanism in which the second equivalent C-H activation of benzene is the rate-determining step.

Experimental details

NMR spectra were recorded on a Varian 500 MHz NMR spectrometer and referenced to residual solvent peaks (δ = 5.32, 7.16 and 7.26 ppm for CD$_2$Cl$_2$, CDCl$_3$ and C$_6$D$_6$, respectively). Chemical shifts and coupling constants are reported in ppm and Hz, respectively. High resolution mass spectra were recorded on a HP 5970 GC-MS mass spectrometer. The yield of biphenyl and other products were determined by analysing the product solutions on a GC instrument (Agilent 6890N) equipped with a FID detector and DB-5 capillary column of dimensions 0.25 mm ID × 0.25 μm × 30 m. Biphenyl was identified by its retention time in comparison with an authentic sample. Each peak of the GC chromatogram was properly integrated and the actual concentration of biphenyl was obtained from a pre-calibrated plot of peak area versus concentration. All reactions were conducted without taking precautions to exclude air or moisture. Yields and concentrations of product in crude reaction mixtures were determined by calibrated GC analyses after the addition of bromobenzene as internal standard and subsequent aqueous workup.

All commercial reagents and solvents were purchased from Sigma-Aldrich and Fisher Scientific and used as received unless otherwise indicated. [PtMe(bhq)(SMe$_2$)] was prepared according to literature[21] and its purity was checked by ^{1}H NMR and elemental analysis. Benzene was dried and degassed using a Solvent Drying System (Pure Process Technologies,

LLC) and stored over activated molecular sieves. Plastic, disposable syringes were used for measuring solutions volumes.

General procedure for Pt-catalyzed homocoupling of benzene

To a 10.0 mL pressure vessel, benzene (3.0 mL, 34 mmol), $PhI(OAc)_2$ (60 mg, 0.18 mmol) and Pt complex **1** (5.0 mg, 0.013 mmol) were added. The mixture was heated for 24 h at 100 °C in an oil bath. The reaction was cooled to room temperature. The reaction mixture was extracted with 3.0 mL of hexane and filtered through a Silica gel column to afford biphenyl up to 30% yield. Small amounts of PhOAc and terphenyl derivatives were also observed as additional co-products.

General procedure for kinetic measurements

$[PtMe(bhq)(SMe_2)]$ was measured from a 0.025 M stock solution (112.5 mg Pt complex dissolved in 10.0 mL benzene or benzene-d^6) using a Hamilton gastight syringe and transferred into a J-Young NMR tube as container. To the NMR tube containing Pt catalyst, $PhI(OAc)_2$ as a solid (see Tables S4-S6 for required amount) was added, followed by C_6F_6, C_6H_6/C_6D_6 (with dielectric constants of 2.1 and 2.2, respectively; total volume in the NMR tube was 0.60 mL; see Tables S4-S6 for the ratio used for C_6H_6 or C_6D_6 and C_6F_6). C_6F_6 and C_6H_6 have the same polarity. The sum of the volumes of C_6H_6 and C_6F_6 (see Supporting Information) was held constant during these experiments in order to minimize solvent effects on the observed rates. The tightly sealed NMR tube was heated to 100 °C in a preheated oil bath. After the desired reaction time (See Tables S4-S6 for required time), the reaction was quenched by immersing the NMR tube into a liquid nitrogen bath until the solution froze and subsequently the NMR tube was allowed to warm up to room temperature. The reaction mixture was diluted with 1.0 mL of hexane and filtered through a Silica gel column. 10 μL of phenyl bromide as GC internal standard was added. The filtrate was analysed by GC-FID. Yields and concentrations of biphenyl were used to obtain initial rates, which were plotted

versus concentrations of reagents, benzene, PhI(OAc)$_2$ and Pt catalyst. A non-linear least squares method was used to fit the rate data to the equation Rate = $k_{obs} \times$[reagent]^n. Kaleidagraph program was used for data fitting.

Computational details

All calculations were performed using Gaussian 09 software.[22] B3LYP functional was used in combination with 6-31+G* basis set for all main group elements, except Pt and I for which the LANL2DZ basis set was used.[23] Where stated, single point energy calculations conducted at B3LYP with def2-QZVP along with the corresponding ECP (Pt, I) and 6-311+g(2d,p) basis sets. Benzene was chosen as solvent and calculations were carried out using the CPCM model. The stationary points and transition states were characterized by full vibration frequencies calculations, with no imaginary frequency for minima (stationary point), and one imaginary frequency for transition states. Cartesian coordinates and energy of optimized structures are reported in the Supporting Information.

Crystallographic data

Single crystal X-ray diffraction data for complex **4** was collected on a Bruker KAPPA APEX II diffractometer equipped with an APEX II CCD detector using a TRIUMPH monochromator with a Mo Kα X-ray source (k = 0.71073 Å). The crystal was mounted on a cryoloop under Paratone-N oil and kept under nitrogen. Absorption correction of the data was carried out using the multiscan method SADABS.[24] Subsequent calculations were carried out using SHELXTL.[25] Structure determination was done using intrinsic methods. Structure solution, refinement, and creation of publication data was performed using SHELXTL. Crystallographic information is presented in Table S1. Crystallographic data for the structural analysis has been deposited with the Cambridge Crystallographic Data Centre, No. CCDC 1585182. Copies of this information may be obtained free of charge from: The Director,

CCDC, 12 Union Road, Cambridge, CB2 1EZ, UK. Fax: +44(1223)336-033, e-mail: deposit@ccdc.cam.ac.uk, or via the web at www.ccdc.cam.ac.uk.

Results and discussion

Platinum based organometallic chemistry has a rich history and its cyclometalated complexes are readily prepared from simple Pt(II) starting compounds.[26] C–H bond activation of arenes by Pt[27-30] and other metals[1, 2, 9, 15-17] has been reported previously. Coupling of two arenes through reductive elimination on Pt is precedented and well documented.[21, 31-33] Therefore, platinum complexes make good candidates for biaryl synthesis from arenes given a suitable oxidant. We investigated initially the reaction of **1** in the presence of benzene with PhI(OAc)$_2$ as an oxidant. At optimal conditions (see supporting Information, Table S2), we identified that at 100 °C complex **1** and PhI(OAc)$_2$ in benzene afford biphenyl in modest yields 30% relative to PhI(OAc)$_2$, the limiting reagent (see Figure S1). Only catalyst **1** and oxidant are needed, additional acid or co-catalyst not required. A control experiment in the presence of oxidant but absence of Pt catalyst showed no biphenyl product formation (see Table S2, entry 4). The reaction is also carried out in the presence of acetic acid which showed the formation of biphenyl (Table S2, entry 2). As will be discussed later, HOAc has an inhibitory effect on the initial rate of biphenyl formation. Other transition metal catalysts[1] such as Pd(OAc)$_2$[4, 34, 35] and HAuCl$_4$[8] also catalyse aryl homocoupling to biaryl. However, these require electron-rich arenes and in most cases acetic acid and solvent. It is also noteworthy that our protocol can be carried out open to air; it is not necessary to use inert atmosphere.

Time resolved ^{1}H NMR spectra of the reaction of PhI(OAc)$_2$ as oxidant and [PtMe(bhq)(SMe$_2$)], **1** at 100°C in C$_6$D$_6$ are shown in Figure 1. The signals for PhI(OAc)$_2$ diminished over the course of 20 h and the signals for PhI increased. The peaks in the phenyl

region are clean and only due to PhI because the biphenyl product is deuterated and this not observable in the ^{1}H NMR spectrum. After heating for 20-24 at 100 °C in an oil bath, the reaction was cooled to room temperature and extracted with 3.0 mL of hexane and filtered through a Silica gel column to afford biphenyl-d^{10}. The biphenyl-d^{10} product and small amounts of PhOAc and terphenyl derivatives (as additional co-products) were observed and identified by GC-MS analysis.
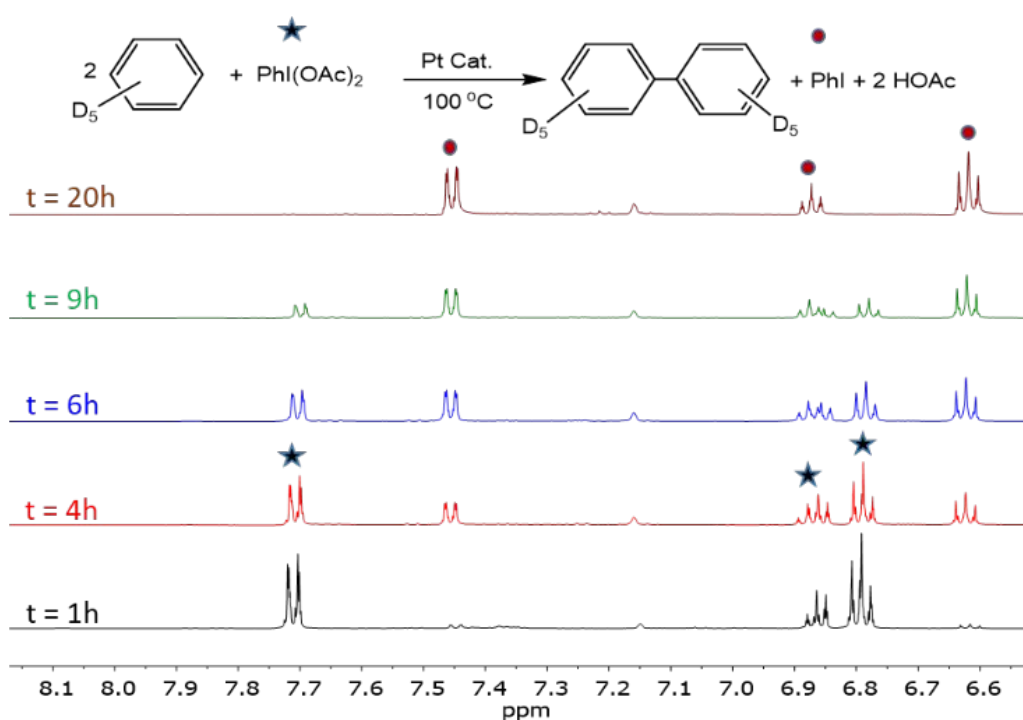
Figure 1. ^{1}H NMR spectra of the reaction of PhI(OAc)$_2$ and [PtMe(bhq)(SMe$_2$)], **1** in C$_6$D$_6$ at 100 °C; condition: [**1**] = 0.010 M, [PhI(OAc)$_2$] = 0.15 M in C$_6$D$_6$ (1.0 mL). Only aromatic region is shown.

A full time kinetic profile for homocoupling of benzene to biphenyl is shown in Figure 2A. To obtain the order of the reaction with respect to each of the species present in the reaction mixture, the following experiments were done.

Order in catalyst [PtMebhq(SMe$_2$)], 1. Reaction order with respect to Pt catalyst concentration [1] was determined using initial rates method over the concentration range 2.0-12.6 mM (see Table S4 and Figure S2). The concentration of biphenyl as determined by quantitative GC-FID was used to obtain initial rates. In determining the order in catalyst, [benzene] = 5.6 M and [PhI(OAc)$_2$] = 0.20 M were used. C$_6$F$_6$ was used as a co-solvent. C$_6$F$_6$ and C$_6$H$_6$ (with dielectric constants of 2.1 and 2.2, respectively) have the same polarity. The sum of the volumes of C$_6$H$_6$ and C$_6$F$_6$ (see Supporting Information) was held constant during these experiments in order to maintain polarity and to minimize solvent effects on the observed rates.[36] A plot of initial rate versus [1] (Figure 2B) was linear with a power dependence on [Pt][a] of 0.97 ± 0.07, in agreement with a first-order dependence on catalyst over the concentration range employed.

Order in oxidant PhI(OAc)$_2$. The dependence on oxidant PhI(OAc)$_2$ was determined at [PhI(OAc)$_2$] = 0.18-0.75 M, [1] = 4.2 mM and [C$_6$H$_6$] = 5.6 M in C$_6$F$_6$ as co-solvent (see Figure 2C, Table S5, and Figure S3). The initial rate was constant and independent of PhI(OAc)$_2$. Therefore, the order in oxidant PhI(OAc)$_2$ is zero-order.

Order in benzene. In order to determine the order of reaction in benzene, initial rate of reaction was over varying concentrations of benzene (see Figure 2D, Table S6, and Figure S4). As evident from Figure 2D, the initial rate dependence on [benzene] is quadratic with power coefficient of 2.2 ± 0.2. Hence, the reaction is second-order in benzene.
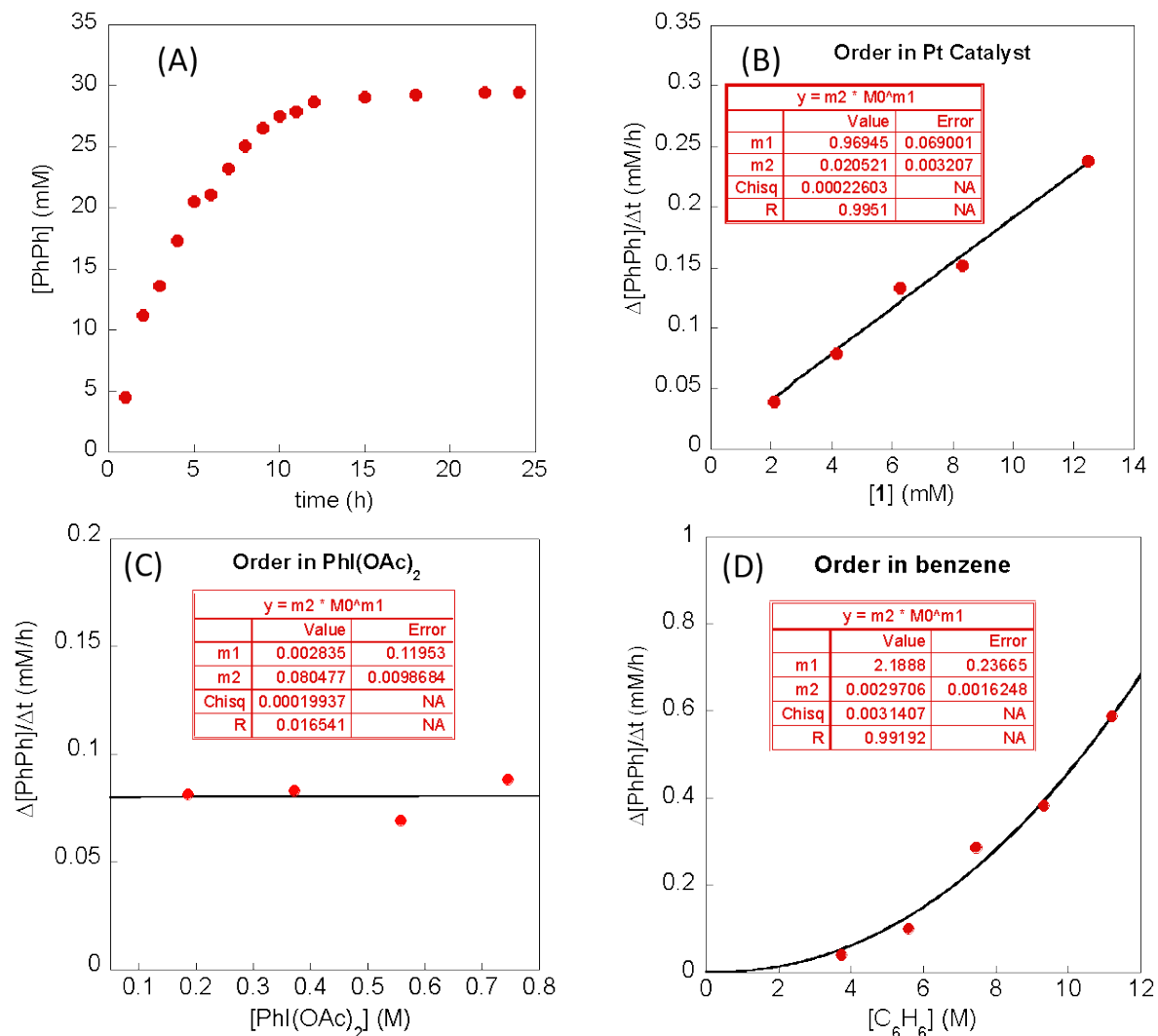
Figure 2. (A) Change in biphenyl concentration over time; [**1**] = 4.2 mM, [C_6H_6] = 5.6 M, [PhI(OAc)$_2$] = 200 mM. (B) Plot of initial rate versus concentration of Pt catalyst, **1**: [**1**] = 2.0-12.6 mM, [C_6H_6] = 5.6 M, [PhI(OAc)$_2$] = 200 mM with C_6F_6 as co-solvent. (C) Plot of initial rate versus concentration of PhI(OAc)$_2$ oxidant: [PhI(OAc)$_2$] = 0.18-0.75 mM, [**1**] = 4.2 mM, [C_6H_6] = 5.6 M. (D) Plot of initial rate versus concentration of benzene: [C_6H_6] = 3.7-11.2 M, [**1**] = 4.2 mM, [PhI(OAc)$_2$] = 200 mM.

Kinetic Isotope Effect (KIE). The kinetic isotope effect (KIE) was determined by comparing the initial reaction rate of C_6D_6 with C_6H_6. A plot of KIE (k_H/k_D) is shown in Figure 3 from which a KIE value of 3.4 ± 0.1 was obtained. This value is consistent

with a primary kinetic isotope effect in which C-H bond breaking is part of the rate-determining step.[36]
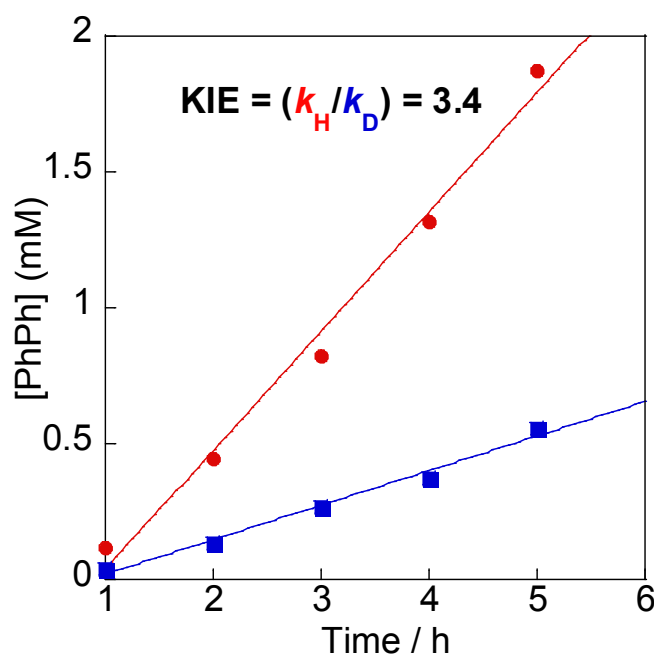
Figure 3. Kinetic isotope effect derived from initial rate measurements for coupling of benzene to form biphenyl using $PhI(OAc)_2$ as oxidant and Pt complex **1** as catalyst; [benzene] = 5.6 M, [**1**] = 12.6 mM, [$PhI(OAc)_2$] = 200 mM.

Working mechanistic hypotheses and catalyst speciation. Based on the data presented so far, three different mechanisms for homocoupling of benzene to biphenyl can be proposed (Schemes 1 and 2). The first possible mechanism (Scheme 1, Path **A**) is the initial oxidation of Pt(II) complex **1** by $PhI(OAc)_2$, followed by reductive elimination of MeOAc and rapid oxidation of complex **3** to give the active Pt(IV) catalyst **IMa**. The latter oxidizes benzene through two consecutive C-H activation steps to give the Pt(IV) diphenyl complex **IMb**. The catalytic cycle completes via reductive elimination of biphenyl regenerating complex **3**.

Two alternative mechanisms are shown in Scheme 2 as pathways **B** and **C**. The second mechanism (Scheme 2, Path **B**) features two consecutive C-H activation steps by Pt(II) complexes to eventually form a diphenyl platinum(IV) complex, followed by C-C coupling to give biphenyl. The third mechanism (Scheme 2, Path **C**) includes the initial C-H activation of benzene by Pt(II) complex **3**, followed by oxidation to give **IMb**. The Pt(IV) complex **IMb** proceeds via a second C-H activation to give a Pt(IV) diphenyl complex, which eliminates biphenyl to complete the cycle.

The proposed mechanism in Scheme 1 involves intermolecular benzene activation at Pt(IV) and C-C reductive elimination. In the first step, Pt(II) complex **1** reacts with PhI(OAc)$_2$ to give cycloplatinated(IV) complex, **2**, which undergoes C-O reductive elimination process to give the catalytically relevant complex [Ptbhq(OAc)(SMe$_2$)], **3**.[37] The chemistry leading to complex **3** can be considered activation and maybe responsible for the observed induction period as seen in Figures S2-S4. Complex **3** can also be formed by reaction of complex **1** with HOAc, independent of PhI(OAc)$_2$ (see Supporting Information for experimental details). Complex **3** was characterized by ^{1}H NMR (in CDCl$_3$: δ 2.10 (s, methyl of OAc group, 3H), 2.86 (s, $^3J_{PtH}$ = 53.8 Hz, SMe$_2$ *trans* to N, 6H),[21, 37] 9.86 (d, J_{HH} = 7.0 Hz, $^3J_{PtH}$ = 38.7 Hz, the C–H proton adjacent to N of bhq, 1H), other aromatic protons of bhq ligand: 7.51–8.42). **3** reacts rapidly with PhI(OAc)$_2$ at 100 °C to give platinum(IV) complex **IMa**, which is proposed to be the active catalyst for C-H activation. The first benzene molecule reacts with **IMa** to form complex **IMb** by releasing HOAc. The reaction of a second molecule of benzene with **IMb** is the rate-determining step (RDS), which is consistent with the experimental finding of second-order dependence on benzene. The product is diphenyl cycloplatinated(IV) compound **IMc**, which is the complex responsible for C-C bond formation via reductive elimination.

To probe more closely the transformation of **IMb** → **IMc** and C-C reductive elimination, we prepared [PtPh(bhq)(SMe$_2$)], **4**, independently by reaction of PtPh$_2$(SMe$_2$)$_2$ with benzo[h]quinole,[38] (see Figure 4 for its structure) and examined the stoichiometric reaction between **4** and PhI(OAc)$_2$ in C$_6$D$_6$. ^{1}H NMR and GC-MS analysis (see Supporting Information; Figures S5 and S6) showed the formation of half deuterated biphenyl (C$_6$H$_5$-C$_6$D$_5$) with molecular mass of 159 m/z. However, the Pt(IV) complexes **IMb** and **IMc** were very challenging to isolate or detect in the reaction mixture. It should be noted that independently synthesized complexes **3** (prepared by the reaction of complex **1** with HOAc) and **4** (synthesized independently by reaction of PtPh$_2$(SMe$_2$)$_2$ with benzo[h]quinole) were tested as catalysts and found to be competent in coupling benzene to biphenyl in the presence of PhI(OAc)$_2$ (see Scheme 1 and Figures S7 and S8). Control reactions with complexes **1**, **3** and **4** in the absence of oxidant do not produce biphenyl. Additional control reactions between these complexes (**1**, **3**, and **4**) and benzene (in the absence of PhI(OAc)$_2$) at 100 °C showed no observable change and the complexes were stable in benzene (see Supporting Information for experimental details and Figures S12-13). C-H activation by Pt(II) complexes could proceed to undetected steady-state intermediate. Therefore, we investigated H/D exchange with Pt(II) complexes and observed no isotope exchange (see Supporting Information, Figures S14-17). All of these control experiment point to Scheme 2, pathways B and C, as an unlikely pathway.

On the other hand, Pt(II) complexes **1**, **3** and **4** react readily with PhI(OAc)$_2$ in benzene or any inert organic solvent such as CH$_2$Cl$_2$ (see Supporting Information, Figures S9-11). These observations provide reasonable evidence that Pt(IV) such as complexes **IMa**, **IMb** and **IMc** are responsible for C-H activation and on the catalytic path as shown in Scheme 1. A similar mechanism was suggested by Sanford[29] et. al.

for C-H arylation of naphthalene by Na_2PtCl_4. C-H activation of arene by Pt(IV) complexes to give arylplatinum(IV) complexes has been reported.[39] C-H bond activation by Pt (IV) complexes is commonly observed and proceeds through a key five coordinate intermediate accessed through ligand loss from the ground-state octahedral Pt(IV) structure.[29, 39, 40]

An alternative mechanism in which the biphenylplatinum complex is formed by disproportionation or transmetalation of two phenylplatinum complex is also a possibility. The transmaetalation mechanism has been considered for Pd-catalyzed oxidative coupling of some arenes through the formation of diarylmetal species.[10, 41] This mechanism for our study is ruled out because initial rates of the reaction would reveal a second-order dependence on Pt concentration for transmetalation mechanism. On the other hand, an unusually large deuterium kinetic isotope effect (KIE) will be obtained when transmetalation mechanism is occurred. For example, KIE value of 24 ± 2 is reported for Pd-catalyzed aerobic oxidative coupling of benzene.[10] Therefore, KIE of 3.4 ± 0.1 in Figure 3, obtained for Pt-mediated benzene C-H activation, is not unusual and fits in the range expected for a monometallic mechanism when first C-H activation is rate-determining step.

Scheme 1. Proposed Mechanism (path **A**) of the Pt-Catalyzed Benzene Coupling to

Biphenyl.

Scheme 2. Two Alternative Mechanisms for Homocoupling of Benzene to Biphenyl
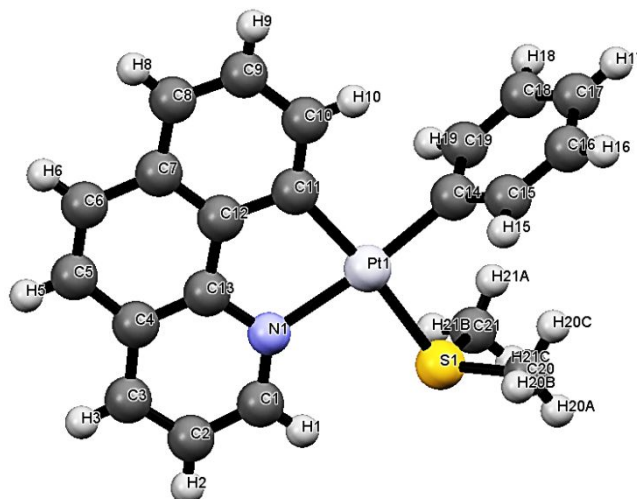
Figure 4. Structure of complex **4** (crystal suitable for X-ray crystallography was obtained by slow evaporation of its solution in C_6H_6 at room temperature). Selected bond distances (Å) and angles (°): Pt(1)-N(1) 2.128(6); Pt(1)-S(1) 2.3584(18); C(14)-Pt(1) 2.009(7); C(11)-Pt(1) 2.030(7); C(14)-Pt(1)-C(11) 93.0(3); C(14)-Pt(1)-N(1) 173.9(2); C(11)-Pt(1)-N(1) 81.5(3); C(14)-Pt(1)-S(1) 92.90(19); C(11)-Pt(1)-S(1) 173.5(2); N(1)-Pt(1)-S(1) 92.46(16).

The co-product of benzene coupling is PhI, which presumably comes from PhI(OAc)$_2$. One may suggest that the source of phenyl groups in biphenyl could be PhI. The following experiments demonstrate that benzene is the source of biphenyl (the conditions used for these experiments are the same as those described for C_6H_6 in experimental details):

1) When the experiment is performed in C_6D_6 (instead of C_6H_6) and $C_6H_5I(OAc)_2$, only biphenyl-d^{10} is observed (see Figures 5 and S13).

2) The reaction with PhI(OAc)$_2$ at 100 °C (in the absence of benzene) does not produce biphenyl (note that at higher temperature, e.g. 140 °C, iodinated biphenyl products were observed).

3) The experiment with toluene instead of benzene produced only derivatives of toluene coupling (Me-C_6H_4-C_6H_4-Me) and biphenyl (C_6H_5-C_6H_5) was not observed (see Figure S19).
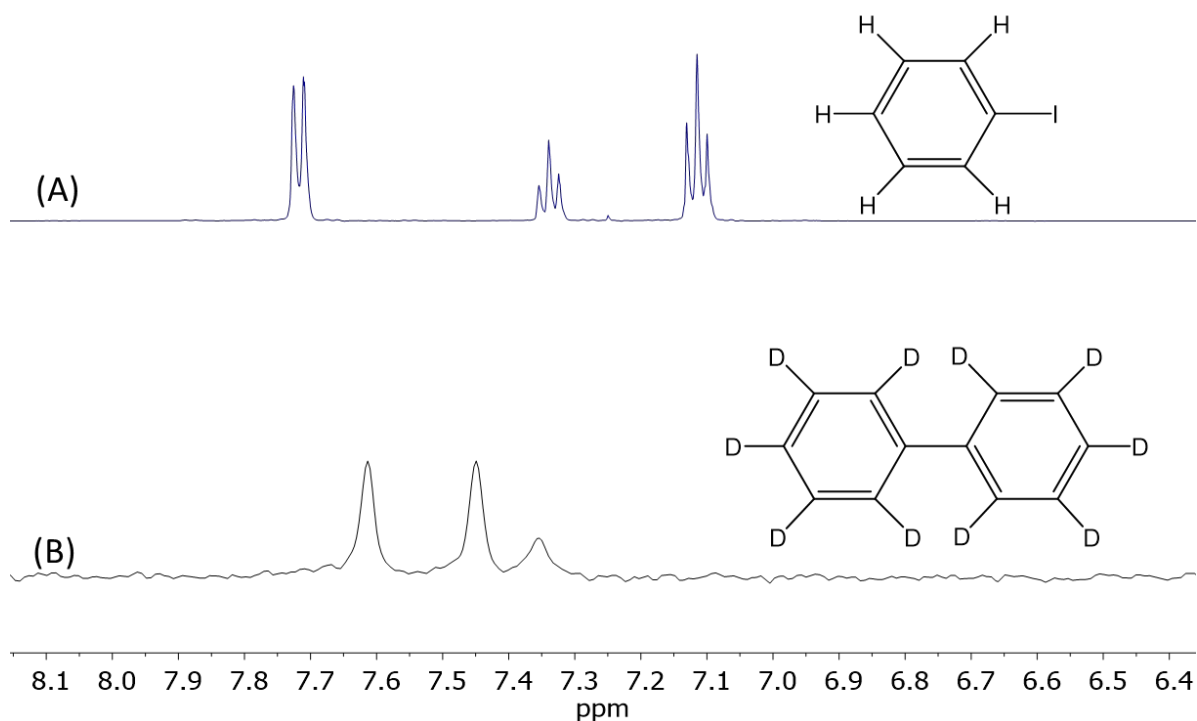
Figure 5. (A) ^1H and (B) D NMR spectra of benzene-d^6 coupling to give exclusively biphenyl-d^{10} in CD_2Cl_2 (A) and CH_2Cl_2 (B): reaction conditions: [Pt catalyst] = 0.010 M, [PhI(OAc)$_2$] = 0.18 M in 1.0 mL C_6D_6 at 100 °C after 24 h.

Based on the catalytic cycle shown in Scheme 1, the rate equation can be written as shown in eq. 1 (see supporting information for derivation).

$$\frac{d[PhPh]}{dt} = \frac{k_1 k_2 [PhH]^2 [Pt]_T}{k_{-1}[HOAc] + (k_1 + k_2)[PhH]} \qquad (1)$$

If we suppose that the second C-H activation step is rate-determining (eq. 2), we obtain the rate law shown in eq. 3.

$$k_{-1}[HOAc] \gg (k_1 + k_2)[PhH] \qquad (2)$$

$$\frac{d[PhPh]}{dt} = \frac{k_1 k_2 [PhH]^2 [Pt]_T}{k_{-1}[HOAc]} \quad (3)$$

The rate equation shown in eq. 3 is fully consistent with the experimental data. It predicts first-order in Pt, second-order dependence in benzene, and zero-order in PhI(OAc)$_2$. As expected a primary KIE is found showing C−H activation is part of the RDS. The inverse dependence of the initial rate of biphenyl formation on the concentration of HOAc would also support our proposed mechanism. As shown in Figure 6 (see also Figure S20 for GC-MS data), initial rate decreases from 0.071 ± 0.001 mM/h in the absence of HOAc to 0.042 ± 0.001 mM/h in the presence of 80 mM HOAc. Using the initial rate, shown in Figure 6, the value of rate constant k (= $K_1 k_2$) is 7.1×10^{-9} L mol^{-1} s^{-1}. Carboxylic acids such as acetic acid and trifluoroacetic acid are usually used as the solvent in biaryl formation.[1] For example Tse et. al. have used[8] acetic acid as a good solvent for oxidative homocoupling of arenes using PhI(OAc)$_2$ and a gold complex as oxidant and catalyst, respectively. Also Serena and Corma used[42] supported gold nanoparticles for production of biphenyl using decane as a good solvent. They found that solvents such as acetone or acetic acid are unsuitable and no biaryl formation was observed.
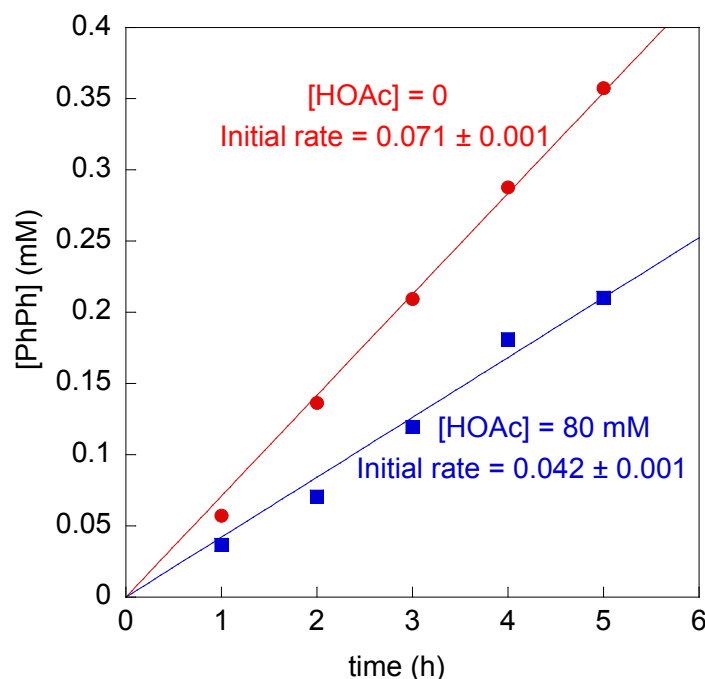
Figure 6. Effect of HOAc on the rate of the coupling of benzene to biphenyl; $[C_6H_6]$ = 5.6 M, [**1**] = 4.2 mM, $[PhI(OAc)_2]$ = 200 mM.

DFT investigation of the reaction mechanism. Density functional theory (DFT) calculations were conducted to provide insight regarding our proposed mechanism. We focused our study on the C-H bond activation and C-C bond formation steps (see Figure 7). Several processes were explored for metalation of benzene with Pt(IV) compound **IMa**, anticipating the need for a vacant coordination site. All possible isomers of complex **IMa** were examined and compound **IMa1** (see Figure 7) was most favoured energetically (Figure S21 shows all possible isomers). Further consideration of the mechanism was limited to steps subsequent to $[Pt(bhq)(SMe_2)(OAc)_2](OAc)$, **IMa1**. The computed free energy profile for proposed mechanism is shown in Figure 7. Compound **IMa1** is envisaged to form directly via dissociation of an acetate ion *trans* to carbon in $[Pt(bhq)(SMe_2)(OAc)_3]$ (see Scheme 1). This OAc^- dissociation is enhanced by the *trans* influence of the carbon atom. Isomerization of this 5-coordinate Pt complex gives intermediate **IMa7**, which isomerizes to **IMa5**. This Pt(IV) cationic intermediate reacts with free benzene to form **TSAB2** containing Pt···C (2.22 Å),

C···H (1.21 Å) and O···H (1.53 Å) interactions prior to formation of **IMb2** (see Figure 8). The free energy barrier for the first C-H activation of benzene is 32.8 kcal mol^{-1}. This value is quite close to previously reported values (26.4 and 29.6 kcal mol^{-1}) for C−H activation of o-xylene and naphthalene on Pd(TFA)(OAc)[10] and Na$_2$PtCl$_4$[40], respectively. After isomerization of **IMb2** to **IMb3** (in which the OAc$^-$ is located *trans* to the C atom), intermediate **IMb3** undergoes a second C-H activation step to form intermediate **IMc1** through transition state **TSBC** (see Figure 8). This transition state contains Pt···C (2.24 Å), C···H (1.21 Å) and O···H (1.53 Å) interactions comparable with those calculated for **TSAB2**. The energy barrier for the second C-H activation step is calculated to be 36.3 kcal mol^{-1}, higher than the energy barrier for the first C-H activation, which is consistent with the observed second-order dependence on benzene. The acetate ion (as seen in **TSAB2** and **TSBC**) assists in C-H activation of benzene. The phenyl groups in **IMc1** are *cis* with respect to each other, which is necessary for C-C reductive elimination. Biphenyl is formed from intermediate **IMc1** through **TSCA2** (see Figure 8) giving complex **3** and completing the catalytic cycle. The energy barrier for Ph-Ph coupling is 29.7 kcal mol^{-1}, which is lower than 36.3 kcal mol^{-1} for C-H activation showing that the latter is rate determining, in agreement with experimental findings.

As shown in Figure 6 and based on eq. 3, the rate constant k (=K_1k_2) is found to be 7.1×10^{-9} L mol^{-1} s^{-1}. Considering the calculated activation free energy values of 32.8 and 27.6 kcal mol^{-1} for the forward and reverse reactions (see Figure 7 and Scheme 1, **3**→**IMb2**), and the value of 31.0 kcal mol^{-1} for the second C-H activation step (**IMb3**→**TSBC**) at the same condition, the values of k_1, k_{-1} and k_2 are calculated to be 4.6×10^{-7}, 5.1×10^{-4} and 5.2 ×10^{-6} s^{-1}, respectively. From these values, DFT-calculated value of k (=k_1k_2/k_{-1}) is obtained as 4.7×10^{-9} L mol^{-1} s^{-1} which is in very good agreement with the experimental value of 7.1×10^{-9} L mol^{-1} s^{-1}. Furthermore, the experimental value of the free energy of activation $\Delta G^{\ddagger}_{exp}$ = 35.9 kcal mol^{-1}

is in excellent agreement with the calculated $\Delta G^{\ddagger}_{calc.} = 36.2$ kcal mol^{-1} ($\Delta G^{\ddagger} = \Delta G^{\ddagger}_{1} - \Delta G^{\ddagger}_{-1} + \Delta G^{\ddagger}_{2}$; see Figure 7) in the same condition. The net free energy change for formation of biphenyl from benzene is exergonic -89.3 kcal mol^{-1}.
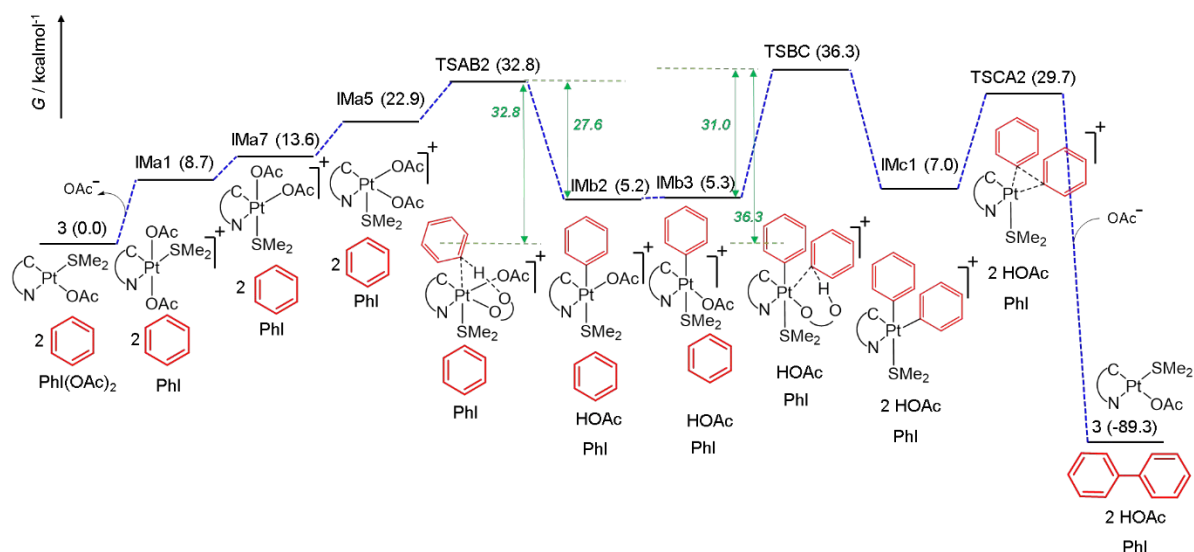
Figure 7. Computed free energy (kcal mol^{-1}) pathway for Pt-catalyzed formation of biphenyl from benzene. Structures optimized at B3LYP level with lanl2dz (Pt, I) and 6-31+G* basis set and a solvent correction (benzene, CPCM). The energy barrier for oxidation of **3** to IMa1 by PhI(OAc)$_2$ was calculated to be 12.2 kcal mol^{-1}.
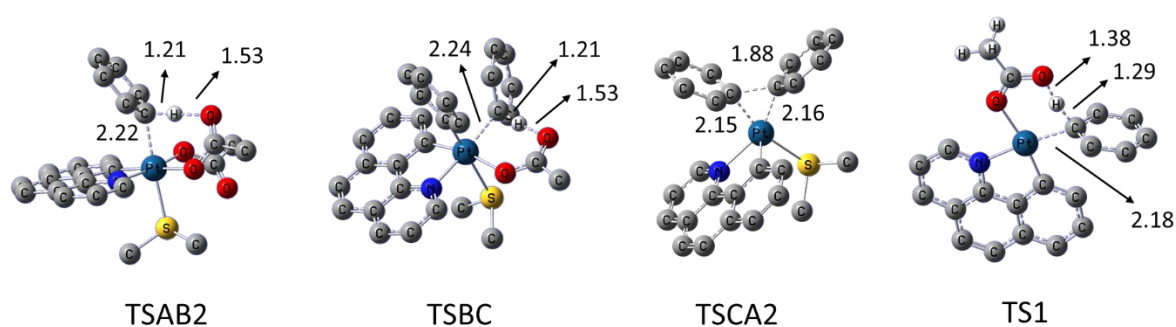
Figure 8. Structures of suggested transition states during Pt-catalyzed formation of biphenyl from benzene. Selected bond distances (Å) are shown.

The mechanisms shown in Scheme 2 were ruled out because it was shown that no reaction took place between Pt(II) complexes **3** and **4** with benzene. As explained before, control reactions with Pt complexes **3** and **4** in the absence of PhI(OAc)$_2$ do not form biphenyl. Additional control reactions between these complexes (**3** and **4**) and benzene (in the absence of PhI(OAc)$_2$) also showed that the complexes were stable in benzene (see Figures S12-13). These observations have been also proven by investigation of H/D exchange with Pt(II) complexes, observing no isotope exchange (see Figures S14-17). Density functional theory (DFT) calculations were used to provide more insight into the suggested mechanisms; Paths **B** and **C** in Scheme 2. We focused on the C-H activation step in both pathways (see SI for details on path **B**). In the first step (**3** + Ph-H → **4** + HOAc) which is a common step in two alternative mechanisms, complex **3** reacts with benzene to give Pt(II)-Ph complex **4** through transition state **TS1** (see Figure 8 for its structure) in which C-H activation of the first incoming benzene molecule occurs with an energy barrier of 30.3 kcal mol^{-1}. This value is close to the 26.4 kcal mol^{-1} reported for the C−H activation step of o-xylene using Pd(TFA)(OAc).[10] Comparing the value of 30.3 and 12.2 kcal mol^{-1} for reaction of **3** with benzene and PhI(OAc)$_2$, respectively, show that complex **3** reacts more readily with the oxidant than benzene.

Conclusion

We have reported the first platinum catalyst for coupling of benzene to biphenyl. Cycloplatinated(II) complex [PtMebhq(SMe$_2$)], **1**, reacts with PhI(OAc)$_2$ to form Pt(IV) [Pt(bhq)(OAc)$_2$(SMe$_2$)(OAc)], **IMa**, which is the active catalyst for breaking the C–H bond in benzene. Complex **3** was separated from the reaction mixture, characterized spectroscopically, and demonstrated to be a competent catalyst in biphenyl formation from

benzene. It should be noted, however, that **3** is not stable over prolonged periods of time and it decomposes to Pt metal. Also reaction of PhI(OAc)$_2$ with [Pt(C$_6$H$_5$)(bhq)(SMe)$_2$], **4**, in C$_6$D$_6$ at 1:1 stoichiometric ratio, gives exclusively C$_6$H$_5$-C$_6$D$_5$. This result is indirect evidence for the intermediate [PtPh(bhq)(SMe$_2$)(OAc)$_2$] (**IMb** in Scheme 1) along the reaction pathway. Kinetics studies showed first-order dependence on Pt, second-order on benzene, zero-order on oxidant PhI(OAc)$_2$, and inhibition by HOAc. The experimental rate law in conjunction with a primary KIE of 3.4 are consistent with C-H activation on a single Pt site with the C-H oxidative addition of the second benzene molecule being the RDS. The described findings here provide an important foundation for future studies of Pt-catalyzed biaryl coupling reactions.

Conflicts of interest

There are no conflicts to declare.

Electronic supplementary information

Electronic supplementary information (ESI) available: Crystallographic data (CCDC 1585182), experimental details, derivation of rate law and DFT data. For ESI and crystallographic data in CIF or other electronic format see DOI: 10.1039/??????.

Acknowledgments

References

1. Y. Yang, J. Lan and J. You, *Chem. Rev.*, 2017, **117**, 8787−8863 and references therein.
2. I. Hussain and T. Singh, *Adv. Synth. Catal.*, 2014, **356**, 1661-1696.
3. J. P. Barham, G. Coulthard, R. G. Kane, N. Delgado, M. P. John and J. A. Murphy, *Angew. Chem. Inter. Ed.* , 2016, **55**, 4492-4496.
4. Y. Liu, X. Wang, X. Cai, G. Chen, J. Li, Y. Zhou and J. Wang, *ChemCatChem*, 2016, **8**, 448-454.
5. Y. Liu, Y. Zhou, J. Li, Q. Wang, Q. Qin, W. Zhang, H. Asakura, N. Yan and J. Wang, *Appl. Catal. B, Env.*, 2017, **209**, 679-688.
6. M. Schubert, P. Franzmann, A. Wünsche von Leupoldt, K. Koszinowski, K. Heinze and S. R. Waldvogel, *Angew. Chem. Inter. Ed.*, 2016, **55**, 1156-1159.
7. F. Wang, S. Yu and X. Li, *Chem. Soc. Rev.* , 2016, **45**, 6462-6477.
8. A. Kar, N. Mangu, H. M. Kaiser, M. Beller and M. K. Tse, *Chem. Commun.* , 2008, 386-388.
9. M. Hofer and C. Nevado, *Tetrahedron*, 2013, **69**, 5751-5757.
10. D. Wang and S. S. Stahl, *J. Am. Chem. Soc.* , 2017, **139**, 5704-5707.
11. D. Wang, Y. Izawa and S. S. Stahl, *J. Am. Chem. Soc.* , 2014, **136**, 9914-9917.
12. X. C. Cambeiro, N. Ahlsten and I. Larrosa, *J. Am. Chem. Soc.* , 2015, **137**, 15636-15639.
13. J. Kim and S. H. Hong, *ACS Catal.* , 2017, **7**, 3336-3343.
14. A. Kar, N. Mangu, H. M. Kaiser and M. K. Tse, *J. Organomet. Chem.* , 2009, **694**, 524-537.
15. M. Simonetti, G. J. P. Perry, X. C. Cambeiro, F. Juliá-Hernández, J. N. Arokianathar and I. Larrosa, *J. Am. Chem. Soc.* , 2016, **138**, 3596-3606.
16. Y. Liu, Y. Zhou, J. Li, Q. Wang, Q. Qin, W. Zhang, H. Asakura, N. Yan and J. Wang, *Appl. Catal. B.*, 2017, **209**, 679-688.
17. X. Guo, G. Deng and C. J. Li, *Adv. Synth. Catal.*, 2009, **351**, 2071-2074.
18. K. R. Pichaandi, L. Kabalan, H. Amini, G. Zhang, H. Zhu, H. I. Kenttämaa, P. E. Fanwick, J. T. Miller, S. Kais, S. M. Nabavizadeh, M. Rashdi and M. M. Abu-Omar, *Inorg. Chem.* , 2017, **56**, 2145-2152.
19. M. Crespo, M. Martínez, S. M. Nabavizadeh and M. Rashidi, *Coord. Chem. Rev.* , 2014, **279**, 115-140.
20. M. M. Abu-Omar, A. Loaiza and N. Hontzeas, *Chem. Rev.* , 2005, **105**, 2227-2252.
21. M. G. Haghighi, S. M. Nabavizadeh, M. Rashidi and M. Kubicki, *Dalton Trans.* , 2013, **42**, 13369-13380.
22. M. Frisch, G. Trucks, H. B. Schlegel, G. Scuseria, M. Robb, J. Cheeseman, G. Scalmani, V. Barone, B. Mennucci and G. Petersson, *Journal*, 2009.
23. P. J. Hay and W. R. Wadt, *J. Chem. Phys.* , 1985, **82**, 270-283.
24. G. Sheldrick, *SADABS, Empirical Absorption Correction Program; University of Göttingen: Germany, 1997*, 2005.
25. SHELXTL PC, Version 6.12, Bruker AXS Inc., Madison, WI, 2005.
26. M. Albrecht, *Chem. Rev.* , 2009, **110**, 576-623.
27. T. Furukawa, M. Tobisu and N. Chatani, *J. Am. Chem. Soc*, 2015, **137**, 12211-12214.
28. J. A. Labinger, *Chem Rev*, 2017, **117**, 8483-8496.
29. A. M. Wagner, A. J. Hickman and M. S. Sanford, *J. Am. Chem. Soc.* , 2013, **135**, 15710-15713.

30. A. Nahaei, S. M. Nabavizadeh, F. N. Hosseini, S. J. Hoseini and M. M. Abu-Omar, *New J. Chem.*, 2019, **43**, 8005-8014.
31. A. L. Liberman-Martin, D. S. Levine, W. Liu, R. G. Bergman and T. D. Tilley, *Organometallics*, 2016, **35**, 1064-1069.
32. I. Dubinsky-Davidchik, I. Goldberg, A. Vigalok and A. N. Vedernikov, *Angew. Chem. Inter. Ed.*, 2015, **54**, 12447-12451.
33. M. D. Aseman, S. M. Nabavizadeh, H. R. Shahsavari and M. Rashidi, *RSC Adv.*, 2015, **5**, 22692-22702.
34. Y. Izawa and S. S. Stahl, *Adv. Synth. Cat.*, 2010, **352**, 3223-3229.
35. P. Zhao, Y. Leng, M. Zhang, J. Wang, Y. Wu and J. Huang, *Chem. Commun.*, 2012, **48**, 5721-5723.
36. A. K. Cook and M. S. Sanford, *J. Am. Chem. Soc.*, 2015, **137**, 3109-3118.
37. M. D. Aseman, S. M. Nabavizadeh, F. Niroomand Hosseini, G. Wu and M. M. Abu-Omar, *Organometallics*, 2018, **37**, 87-98.
38. S. M. Nabavizadeh, H. Amini, H. R. Shahsavari, M. Namdar, M. Rashidi, R. Kia, B. Hemmateenejad, M. Nekoeinia, A. Ariafard and F. N. Hosseini, *Organometallics*, 2011, **30**, 1466-1477.
39. E. S. Rudakov and G. B. Shul'pin, *J. Organomet. Chem.*, 2015, **793**, 4-16.
40. A. J. Canty and A. Ariafard, *Dalton Trans.*, 2017, **46**, 15480-15486.
41. M. Hirano, K. Sano, Y. Kanazawa, N. Komine, Z. Maeno, T. Mitsudome and H. Takaya, *ACS Catal.*, 2018, **8**, 5827-5841.
42. P. Serna and A. Corma, *J. Catal.*, 2014, **315**, 41-47.

Table of Contents Entry

Discovery and Mechanistic Investigation of Pt-Catalyzed Oxidative Homocoupling of Benzene with PhI(OAc)$_2$

S. Masoud Nabavizadeh, Fatemeh Niroomand Hosseini, Chan Park, Guang Wu and Mahdi M. Abu-Omar

One step synthesis, Air stable catalyst, No co-solvent or co-catalyst, $\dfrac{d[PhPh]}{dt} = \dfrac{k[PhH]^2[Pt]}{[HOAc]}$
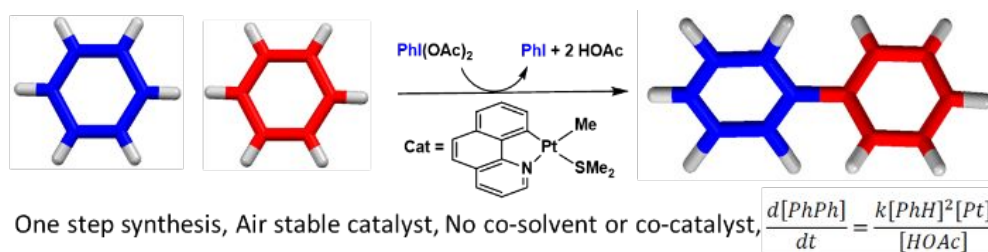
Pt-catalyzed direct coupling of benzene to biphenyl using PhI(OAc)$_2$ as oxidant in the absence of any acid as co-solvent or co-catalyst was mechanistically investigated showing first-order in Pt catalyst and second-order in benzene, which implicates the second C-H activation step as rate-limiting.